



Published in final edited form as:

J Virol Methods. 2008 January ; 147(1): 167–176. doi:10.1016/j.jviromet.2007.08.025.

Quantitative PCR (QPCR) technique for detecting lymphocytic choriomeningitis virus (LCMV) in vivo

Megan M. McCausland and Shane Crotty*

Division of Vaccine Discovery, La Jolla Institute for Allergy and Immunology, San Diego, CA 92121, USA

Summary

Quantitative PCR (QPCR, or real time PCR (rtPCR)) has emerged as a powerful virologic technique for measuring viral replication and viral loads in humans and animal models. We have developed a QPCR assay to accurately quantify lymphocytic choriomeningitis virus (LCMV) in infected mice. We first validated this assay using plasmid DNA and LCMV viral stocks. We then demonstrated that the LCMV QPCR assay can detect LCMV in serum and tissues of chronically infected mice (LCMV-clone 13), with greater sensitivity than conventional plaque assay. Subsequently, we demonstrated that the QPCR assay can detect LCMV in tissues of CD40L^{-/-} mice during a low grade chronic infection with LCMV armstrong. Finally, we improved the assay further such that it was approximately 1000-fold more sensitive than plaque assay for detection of the presence of LCMV in tissue.

Keywords

RNA virus; chronic infection; arenavirus; RT-PCR; rtPCR

1. Introduction

Quantitative PCR (QPCR, or real time PCR (rtPCR)) has emerged as a powerful virologic technique for measuring viral replication and viral loads in humans and animal models, in serum and in tissue samples, and both for culturable viruses and non-culturable viruses. The most well known virologic applications of this technique are the measurement of HCV and HIV viral loads in the serum of infected human patients, but QPCR has now been applied to many viral species.

We have developed a QPCR assay to accurately quantify lymphocytic choriomeningitis virus (LCMV) in infected mice. There were several impetuses for developing such an assay. 1) It is known that the sensitivity of LCMV plaque assays is imperfect, as a bioassay (mouse intracranial injection) can detect infectious virus that is undetectable by plaque assay, and there are reports of immunodeficient mouse strains that appear to clear an acute LCMV_{arm} infection by plaque assay, but viral recrudescence is observed at later time points (Bachmann et al., 2004; Thomsen et al., 1996). 2) It is presumed that isolation of LCMV from infected tissues

*Corresponding author: shane@liai.org. Division of Vaccine Discovery, La Jolla Institute for Allergy and Immunology (LIAI), 9420 Athena Circle, La Jolla, CA 92037, USA. (858) 752-6816. Fax (858) 752-6985

Publisher's Disclaimer: This is a PDF file of an unedited manuscript that has been accepted for publication. As a service to our customers we are providing this early version of the manuscript. The manuscript will undergo copyediting, typesetting, and review of the resulting proof before it is published in its final citable form. Please note that during the production process errors may be discovered which could affect the content, and all legal disclaimers that apply to the journal pertain.

is inefficient due to the labile nature of the viral particles, whereas total RNA extraction is generally highly efficient. 3) Some LCMV strains plaque much more poorly than others due to their minimal cytotoxicity to Vero cells. 4) The current LCMV plaque assay technique takes 5 days, whereas a QPCR assay can be done in less than one day. Therefore, given the prevalence of LCMV use in viral immunology and viral pathogenesis research (Buchmeier and Zajac, 1999; Wherry and Ahmed, 2004), a better technique for quantifying LCMV would be highly valuable. Herein we describe our efforts to develop a sensitive and robust QPCR assay for LCMV.

2. Methods

Mice

C57BL/6J (B6) mice and CD40L^{-/-} B6 mice were purchased from the Jackson Laboratory. Five week old mice were used for LCMV_{cl13} experiments. Six to seventeen week old mice were used for LCMV_{arm} experiments. Animals were bred and maintained in an accredited facility at the La Jolla Institute for Allergy and Immunology (San Diego, CA), and the studies reported in this study conform to the principles outlined by the Animal Welfare Act and the National Institutes of Health guidelines for the care and use of animals in biomedical research.

Viruses

Plaque-purified clones of the Armstrong strain of LCMV (LCMV_{arm}) were propagated in BHK-21 cells (ATCC, Manassas, VA) (Ahmed et al., 1984), and tested for biological activity *in vitro* and *in vivo* (Crotty et al., 2006; Graham et al., 2006)(McCausland et al, JI in press). A second passage stock of plaque purified subclone SC3 (LCMV_{arm-sc3}), was used for all LCMV_{arm} experiments. Both genome segments of LCMV_{arm-sc3} were fully sequenced (excluding the short loop domain), and amino acid differences from the original 1988 LCMV_{arm} sequence (Salvato et al., 1989; Salvato et al., 1988; Salvato and Shimomaye, 1989) were as follows: L^{S108T}, L^{S311R}, L^{T1513K}, L^{L1676V}, Gp^{D176N}, Gp^{R177A}, Gp^{A313E}. For acute infections, mice received 1×10^5 PFU LCMV_{arm} in a volume of 0.5 ml (suspended in RPMI-1640) by two intraperitoneal inoculations (i.p.) of 250 μ l each.

Plaque-purified LCMV-clone 13 (LCMV_{cl13}) clones were propagated in BHK-21 cells and tested for biological activity *in vitro* and *in vivo* (Crotty et al., 2006). A second passage stock of subclone SC9 (LCMV_{cl13-sc9}) was used for all LCMV_{cl13} experiments shown. To establish chronic infections, five week old mice received 2×10^6 PFU LCMV_{cl13} by intravenous inoculation (i.v.) via retroorbital injection (0.2 ml). Both genome segments of LCMV_{cl13-sc9} were fully sequenced (excluding the short loop domain) and mutations Gp^{F260L} and L^{K1079Q} were confirmed (Matloubian et al., 1993; Matloubian et al., 1990). Additional changes in LCMV_{cl13-sc9} from the original 1989 sequences were L^{S108T}, L^{T1513K}, L^{H1665N}, L^{V177I}, Gp^{R177A}, and Gp^{A313E}. Note that L^{S108T}, L^{T1513K}, Gp^{R177A}, and Gp^{A313E} were also present in LCMV_{arm-sc3}.

Cell, tissue, and serum preparation

Organ samples were surgically removed and frozen at -80 °C, then weighed and homogenized using an Omni PCR Tissue Homogenizer (Omni). Normal tissue sample sizes were: spleen, 10mg; liver, 50mg; kidney, 50mg; brain, 50mg; lymph node, 5mg. Tissue samples for plaque assays were homogenized in 1ml of phosphate buffered saline (PBS, pH 7.4). Note that treatment of tissues with RNALater (Ambion, USA) prior to homogenization may increase RNA yields. The homogenizer was washed multiple times between each tissue sample. Tissue samples were prepared differently for QPCR (see below).

Single cell suspensions of spleen were prepared by standard gentle mechanical disruption through a 70 μm nylon mesh screen (BD Falcon) using a 3ml syringe plunger (BD Biosciences), followed by removal of red blood cells with ACK Lysis Solution (Biosource).

Bone marrow cells were obtained by surgical removal of both femurs followed by flushing the shaft of each femur using a syringe containing 5 ml cold DMEM + 10% FCS.

LCMV plaque assay

Plaque forming units (PFU) of viral stocks, and serum and tissue samples from infected mice, were determined by five day plaque assay on VeroE6 cells (to titer LCMV_{arm} virus stock) or Vero cells (to titer LCMV_{c113} stock, or serum and tissue samples from chronically infected mice)(Ahmed et al., 1984). Cells were plated the previous day such that they would be 75-90% confluent at time of infection. Monolayers were infected with virus for 60' at 37 °C, and then covered with a 0.5% agarose (Sigma) and complete 1x Medium 199 (Life Technologies) semisolid overlay. Cells were incubated for 4.5 days at 37 °C, 5-8% CO₂. Then an overlay of 0.02% neutral red in 0.5% agarose and 1x complete Medium 199 was added for overnight staining, followed by plaque enumeration on a lightbox.

LCMV viral load quantitative PCR (QPCR)

Samples: To obtain serum samples, whole blood was collected from metafane (LCMV_{c113} infected mice) or isofluorane (healthy mice) sedated animals into 1.5ml tubes by capillary tube rupture of the retroorbital sinus. Heparinized capillary tubes were used (Sigma). Blood samples were then centrifuged for 20 minute at 12000g and 4 °C to separate the serum. Tissue samples were obtained using sterilized surgical tools, and tools were wiped with 70% ethanol between each mouse to prevent viral cross-contamination, and samples from negative control (uninfected) mice were always obtained first. Normal tissue sample sizes were: spleen, 10mg; liver, 50mg; kidney, 50mg; brain, 50mg; lymph node, 5mg. Tissue samples were immediately snap frozen on dry ice at the time of harvest. All serum and tissue samples were frozen at -80 °C until time for RNA extraction.

RNA isolation: RNA was isolated using the RNAaqueous mini spin column based system (Ambion, Austin, TX), which allows for rapid RNA isolation for both RNA sparse and RNA rich samples (serum and tissue samples, respectively). For serum samples, RNA was isolated from 50 μl serum. For tissue samples, RNA was isolated from 5-50mg tissue homogenized in the presence of lysis buffer (~5mm bore Tissuemiser, Fisher Scientific). Extreme care must be taken to avoid cross contamination, particularly at this stage. Therefore, tissue homogenization was done in a laminar flow hood, and the homogenizer was washed once with PBS, followed by once with 10% bleach, and again with PBS. Note: standard washing of the homogenizer with ethanol and PBS between samples is insufficient and results in RNA cross-contamination. RNA was eluted from RNAaqueous spin columns in a volume of 20 μl and purified RNA was frozen at -80 °C until use.

Primers: Original NP primers (NP1 set, no longer used) = NP1-R (S pos. 2868-2889), AAGCTGAAGGCCAAGATCAT; NP1-F (S pos. 2975-2994), GAGGCTTTCTCATCCCAACTAT. New NP2 primers = NP2-R (S pos. 2697-2720), CAGACCTTGGCTTGCTTTACACAG; NP2-F (S pos. 2601-2623) , CAGAAATGTTGATGCTGGACTGC. New GP primers (recommended optimized primers for all current use) = GP-R (S pos. 970-991), GCAACTGCTGTGTTCCCGAAAC. GP-F (S pos. 877-901), CATTCACCTGGACTTTGTCTCAGACTC. Primers were aliquoted and stored at -80 or -40 °C.

cDNA synthesis: 10µl of RNA was used in a 20µl cDNA reaction with SuperScript III Reverse Transcriptase (SSIII)(Invitrogen, Carlsbad, CA) and a gene specific primer at 55 °C for 1 hr (50 °C was used in some experiments). Optimized primers were required to function well at the higher temperatures utilized by SSIII. Original work (Fig. 2-7) was done using non-optimized NP1-R primer. Later work was done using optimized GP-R primer (Fig. 8-9). Extreme care must be taken to avoid any sources of cross contamination. Two negative control samples from uninfected mice are recommended for all assays, as well and H₂O alone no template controls. Reactions were normally set up inside a laminar flow hood possessing a UV light that was turned on when not in use, to destroy potential sources of RNA or DNA cross-contamination. cDNA reaction incubations were done in a programmed MJ thermocycler (PTC-200, MJ Research), to maintain temperature and time consistency between experiments. Use of SSIII for cDNA synthesis was required to obtain the exquisite sensitivity and specificity required for the QPCR to then be able to detect as few as 1 LCMV copy per reaction or as many as 10⁶ LCMV copies, and not inadvertently prime products from the cellular RNAs that vastly outnumber the LCMV genomic RNA.

QPCR reaction: 5µl of cDNA was used as template for a 25µl QPCR reaction (50 µl rxns were sometimes used), using iTaq SYBR Green Supermix with ROX (Bio-Rad, USA), plated in 96 well plate format and run on a GeneAmp 5700 (ABI, Redwood City, CA). Amplification was done for 40 cycles, with each cycle consisting of two steps: 95 °C, 15 sec; 60 °C, 30 sec. All QPCR samples were run in duplicate. Extreme care must be taken to avoid any sources of cross contamination. Plasmid standard curve samples were always handled last, and were never placed directly adjoining wells containing samples of interest. Multiple “No DNA” (5µl H₂O instead of cDNA) samples were always run as negative controls. Two negative control samples from uninfected mice are recommended for all assays, for each tissue. In original experiments (Fig. 2-4), a standard curve was generated using linearized pCITE-NP (Lee et al., 2002), a gift from Juan Carlos de la Torre (Scripps Research Institute, San Diego, CA). In later work (Figs. 1e-g,8,9), standard curves were generated using linearized pSG5-GP plasmid (Lee et al., 2002), a gift from Dr. Juan Carlos de la Torre (Scripps Research Institute, San Diego, CA). Quantitation of the plasmid standard was done by gel electrophoresis (comparing against a series of DNA standards), plasmid copy number was calculated, and then 10-fold serial dilutions of the plasmid were made. Plasmid standard curve samples were then aliquoted for single usage and frozen at -80 °C long term until use in QPCR. In some cases of high tissue viral loads, 1:200 dilutions of cDNA were used in the QPCR.

Data analysis: Standard curve was calculated using the series of duplicate standard samples in Prism 4.0 (GraphPad, San Diego, CA). Standard curves were log-linear over a range of > 10⁵, with high R² values (~98-99%). Sensitivity of the QPCR assay was 1-5 LCMV genome copies per QPCR reaction, based on the standard curve. QPCR reaction was validated to be sensitive and robust out to 35-36 cycles (1 to 5 LCMV genome copies), but products detected beyond 36 cycles were poorly reproducible and generally discarded. Limit of detection was therefore established in each run as the sensitivity of the QPCR at 35 or 36 cycles backcalculated to the original starting material. In addition, specificity was assessed by analysis of melt curves (for nonspecific amplified products) and analysis of samples from uninfected mice and H₂O alone controls. Limit of detection for any given experiment (and tissue) was set using either the limit of QPCR sensitivity or specificity, whichever was more conservative.

Statistical analysis

Tests were performed using Prism 4.0 (GraphPad, San Diego, CA). Statistics were done using two-tailed, unpaired T test with 95% confidence bounds unless otherwise indicated. Error bars are ± one SEM unless otherwise indicated. Geometric means were used for viral load data, where log₁₀ scales were used. Arithmetic means were used for other data.

Plasma cell ELISPOT

Plasma cells were quantitated by the ELISPOT method previously reported (Crotty et al., 2003; Crotty et al., 2006). Sonicated lysate from LCMV-infected BHK-21 cells was used as capture antigen for LCMV-specific ELISPOT. 96-well MAHA N4510 filter plates were used (Millipore, MA). Goat anti-mouse IgG+M+A (Caltag Laboratories, CA)(62.5ul per 10ml) was used as capture antibody for total Ig ELISPOTs. LCMV antigen was UV inactivated (300 mJ in Stratalinker 1800, Stratagene, CA) after overnight coating onto ELISPOT plate. Plates were blocked with DMEM + 10% FCS. Cells of interest were added to the plate in 3x serial dilutions in DMEM + 10% FCS and incubated at 37 °C, 5-8% CO₂, for 5-6 hrs. Biotinylated goat anti-mouse IgG γ (Caltag Laboratories) followed by streptavidin-HRP (Vector Laboratories, CA) was used for detection. AEC was used for spot development. Incubation buffers used PBS + 0.05% Tween-20 + 1% FCS, and wash buffers used PBS + 0.05% Tween-20. ELISPOT plates were scanned by an ImmunoSpot Analyzer and machine counted using a standardized set of digital counting parameters we established in ImmunoSpot 3.2 (C.T.L., Cleveland, OH).

Flow cytometry analysis

Staining for flow cytometry used mAbs to CD4, CD8, CD3, B220, CD44, CD62L, IFN γ , TNF α , IL-2 (eBiosciences, San Diego, CA); polyclonal goat anti-mouse IgG γ (Caltag Laboratories, Burlingame, CA); Fas, CD138 (BD Pharmingen, CA); and FITC-labeled PNA (Vector Laboratories, Burlingame, CA). Cells were fixed in 2% ultrapure formaldehyde (Polysciences, Inc., Warrington, PA) prior to acquisition. Flow cytometry samples were acquired on a FACSCalibur instrument (Beckton Dickinson, San Jose, CA) and analyzed using FlowJo software (TreeStar, San Carlos, CA).

Intracellular cytokine staining

1×10^6 cells were cultured in the absence or presence of the indicated peptide and brefeldin A for 5-6 h at 37 °C. H-2D^b or H-2K^b restricted epitopes were used at 0.2 ug/ml, and I-A^b restricted epitopes at 2 ug/ml. Following staining for surface antigens, cells were fixed and permeabilized with 2% (w/v) paraformaldehyde (PFA) and 0.1% saponin for 15 min, then stained for the intracellular cytokine of interest in the presence of 0.1% saponin and 2% NCS for 30 min. Cells were washed and then fixed in 2% ultrapure formaldehyde (Polysciences, Inc., Warrington, PA).

3. Results

QPCR standard curve development

A standard curve is necessary for accurate quantitation using QPCR. We developed LCMV standard curves based on both the LCMV NP and GP genes, utilizing linearized plasmids containing those genes. 10-fold dilutions of the standard plasmid were made and run in QPCR (Fig. 1a, e). Dilutions titrated out at regular 3.3 cycle intervals, as expected for log₂ PCR amplification of DNA. Confirmation of appropriate PCR product formation was done by melt curve analysis (Fig. 1b,f). Data was then subjected to log-linear analysis to generate a standard curve for calculation of unknowns (Fig. 1c,g). The standard curves regularly exhibited high R² values (> 0.98). We could reproducibly detect as few as 5 copies of plasmid per QPCR reaction.

We next examined the sensitivity of the NP QPCR assay by comparing LCMV genome/ml versus PFU/ml for a LCMV_{arm} viral stock. Standard plaque assays reproducibly gave a titer of 2×10^6 PFU/ml. Since LCMV is an RNA virus, a reverse transcription (RT) cDNA synthesis step is required prior to PCR amplification. An LCMV-specific primer was utilized for this step, and QPCR was subsequently performed. Quantitation of the LCMV viral stock by QPCR

showed that the LCMV_{arm} stock contained 2×10^8 LCMV genomes/ml. Of note, the QPCR quantitation for the viral stock dropped over a period of 12 months, while the PFU/ml quantitation remained very stable (data not shown). This suggests that some of the increased sensitivity of the QPCR over the plaque assay was due to detection of viral ribonuclear particles (RNP) that degraded over time, in addition to detection of LCMV genomes in intact virions.

Analysis of chronic LCMV_{c113} infection

It can be particularly difficult to obtain good plaque assay results in mice chronically infected with LCMV_{c113} (or other chronic strains), and it is unclear how efficient plaque assays are for measuring LCMV viral loads in tissue samples. Therefore, we compared the QPCR assay against the traditional plaque assay when examining LCMV viral loads in serum and multiple tissues during chronic LCMV_{c113} infection of wild type B6 mice. Serum samples were taken from LCMV_{c113} infected mice at 30 to 90 days post-infection. The serum samples were each divided into two aliquots, one of which was used for LCMV QPCR and the other of which was used for an LCMV plaque assay. The QPCR assay was able to detect LCMV_{c113} viremia at day 30, 60, and 90 post-infection, while the conventional LCMV plaque assay was only able to detect viremia at day 30 post-infection (Fig. 2). This reflects approximately a 30-fold increase in sensitivity of the QPCR assay over the plaque assay. In addition, the QPCR assay was able to detect an 85% drop in viral load between day 60 and day 90 ($P < 0.04$). We were also able to efficiently measure differences in LCMV_{c113} viral loads between wildtype and SAP-deficient mice (Crotty et al., 2006).

In a subsequent series of experiments, we measured LCMV_{c113} viral loads in tissues during a chronic LCMV_{c113} infection. Using the QPCR assay, high viral loads were detectable in serum (6×10^5 LCMV RNA/ml), kidney (1×10^7 LCMV RNA/mg), and liver (3×10^5 LCMV RNA/mg) at 30 days post-infection (Fig. 3). In most experiments we could not quantify LCMV RNA levels in the spleens of LCMV_{c113} infected mice because of amplification of nonspecific QPCR products from splenic RNA (data not shown, discussed below).

Demonstration of cryptic infection in CD40L^{-/-} mice

We used the LCMV QPCR assay highly successfully in the context of a LCMV_{c113} infection. We then moved to a more challenging situation: CD40L^{-/-} mice. It has been reported that CD40L^{-/-} mice appear to clear an acute LCMV_{arm} infection by plaque assay, but viral recrudescence is observed at later time points (Bachmann et al., 2004). We therefore examined viral loads in CD40L^{-/-} mice at day 8 (Fig. 4), day 30 (Fig. 5), and day 90 (Fig. 6) after infection with LCMV_{arm}. QPCR and plaque assay were directly compared for each individual mouse and tissue sample by dividing samples into two aliquots for performing both QPCR and plaque assay. At day 8 post-infection, low level LCMV viremia was detected in two of four CD40L^{-/-} mice by both QPCR and plaque assay (Fig. 4a). Higher levels of LCMV were detected in spleen and liver of CD40L^{-/-} mice by QPCR, while by plaque assay LCMV was only detectable in spleen of CD40L^{-/-} mice (Fig. 4b-c). Bigger differences were observed at day 30 post-infection, when virus was effectively undetectable by plaque assay, but LCMV was detectable in CD40L^{-/-} spleen, liver, and kidney by QPCR, though the differences from wild type did not reach statistical significance (Fig. 5). The phenotype was even stronger at day 90 post-infection, when the QPCR assay detected LCMV in kidney and liver of three out of four CD40L^{-/-} mice, and all four mice were positive for LCMV in the spleen by QPCR (Fig. 6). Differences in QPCR viral loads in spleen and liver reached statistical significance ($P = 0.05$, $P < 0.04$). To confirm that the LCMV_{arm} infections gave the expected CD40L^{-/-} immunological phenotypes, we examined LCMV-specific CD8 T cell (IFN γ ⁺ gp33-specific), CD4 T cell (IFN γ ⁺ gp61-specific), plasma cell (anti-LCMV IgG secreting cells), and germinal center B cells during the effector phase (day 8) and memory phase (days 30 and 90). CD40L^{-/-} effector CD4 T cell response was reduced 3-fold (Fig. 7b) as expected (Whitmire et al., 1999), and the

anti-LCMV plasma cell (Whitmire et al., 1996) and germinal center B cell responses were completely ablated (Fig. 7c-d). The effector CD8 T cell response was moderately reduced (Fig. 7a). The CD40L^{-/-} memory CD4 T cell response was affected severely (Fig. 7f,j)(Bachmann et al., 2004), and the memory CD8 T cell response was also reduced by day 90 post-infection (Fig.7i)(Bachmann et al., 2004).

Improving specificity

While we were able to successfully use the QPCR assay to detect LCMV after LCMV_{cl13} infection in wildtype mice and a cryptic LCMV_{arm} infection in CD40L^{-/-} mice, the LCMV QPCR assay had an obvious deficiency: the limit of detection was negatively impacted by the amplification of nonspecific products during late rounds of QPCR amplification (> 30 cycles). This specificity problem was particularly dramatic in spleen tissue samples. This is a difficult problem, because of the complexity of amplifying a small number of LCMV RNA copies in the presence of an enormous excess of cellular RNAs, particularly in situations where one expects only a tiny fraction of the total cells to be infected with LCMV (i.e., several months into an LCMV_{cl13} infection, or any time after day 5 in a potentially low grade LCMV_{arm} infection such as that seen in CD40L^{-/-} mice). These conditions are probably several orders of magnitude more stringent than conventional QPCR assays conditions for cellular genes.

To address this problem, we tested GP primers and new NP primers (“NP2”) for increased specificity (Figs. 8, 9). The new primer sets had comparable sensitivity to the original NP primer set (Fig. 8), and the GP primer set gave significantly better specificity (no amplification of nonspecific products). We then tested the sensitivity and specificity of the LCMV GP QPCR in the context of an LCMV_{arm} infection of wildtype mice (Fig. 9). LCMV_{arm} was clearly detected in lymph node, spleen, and kidney at day 8 post-infection (Fig. 9), with very low levels of LCMV RNA still detectable at day 30 in LCMV_{arm} infected mice but not in uninfected control mice (Fig. 9). Nonspecific products were not observed (as detectable by the PCR product melt curves), demonstrating the increased specificity of the LCMV GP QPCR. This was a 10-100 fold increase in true sensitivity, due to the increased specificity of the QPCR in tissue samples, allowing for accurate quantitation of extremely small amounts of LCMV RNA. For example, in spleen tissue the new limit of detection was in the range of 10 copies/mg (Fig. 9c), compared to approximately 1×10^3 copies/mg using the earlier primers (Fig. 4, 5, 6). For viral RNA loads in lymph nodes, the difference between day 8 and day 30 was significant in both experiments performed ($P < 0.003$); however, the difference in spleen did not reach statistical significance in the two experiments performed.

4. Discussion

We have developed a QPCR assay to accurately quantify lymphocytic choriomeningitis virus (LCMV) in infected mice. There were several impetuses for developing such an assay, as described in the introduction. First, it is known that the sensitivity of plaque assay is imperfect, as a bioassay (mouse intracranial injection) can detect infectious virus that is undetectable by plaque assay, and there are reports of immunodeficient mouse strains that appear to clear an acute LCMV_{arm} infection by plaque assay, but viral recrudescence is observed at later time points (Bachmann et al., 2004; Thomsen et al., 1996). Herein we have shown that we are able to detect the presence of virus by QPCR when it is not detectable by conventional plaque assay. Second, it is expected that isolation of LCMV from infected tissues is inefficient due to the labile nature of the viral particles, whereas total RNA extraction is generally highly efficient. Herein we have shown that the QPCR assay is highly effective at detecting LCMV in tissue samples. Third, some LCMV strains plaque much more poorly than others due to their minimal cytotoxicity to Vero cells. Herein we have shown that the LCMV QPCR assay can be used to detect both acute (LCMV_{arm}) and chronic (LCMV_{cl13}) strains of

virus. Lastly, the current LCMV plaque assay technique takes 5 days, whereas a QPCR assay can be done in less than one day. Therefore, given the prevalence of LCMV use in viral immunology and viral pathogenesis research, this LCMV QPCR assay is of potential value to a variety of laboratories.

In our experiments, LCMV RNA was detectable in wildtype spleens at day 30 post-infection (Fig. 9), which we have interpreted as residual non-infectious virions or viral RNA. A similar result was reported by another group using a different LCMV RT-PCR approach (Roberts et al., 2004). While we did not detect any LCMV genetic material in the form of DNA (QPCR product in the absence of cDNA synthesis) in a few samples tested at day 8 after LCMV_{arm} infection (data not shown), these experiments were not designed to directly test for the possible (though unlikely) presence of LCMV sequence DNA in the murine genomic DNA (Klenerman et al., 1997), since we specifically isolate RNA, not DNA, from tissues. However, clarifying those issues is beyond the scope of this method paper. It has been recently reported that viral genomic RNA can be detected in murine tissues for at least 60 days after VSV infection, using a QPCR-based approach similar to our LCMV QPCR approach (Simon et al., 2007). The observation of persisting VSV genetic material is perplexing, given that VSV is a well accepted lytic virus causing an acute infection. In theory, designing a QPCR specific for viral mRNA specific sequence should resolve whether or not active infection is involved in either the VSV or LCMV case; however, authors of the VSV QPCR study noted that they have been unable to establish a truly specific viral mRNA QPCR, implicating the presence of antigenomic RNAs packaged in virions at some frequency (Simon et al., 2007), which further complicates analysis. It would be interesting to determine whether a similar situation exists with LCMV.

Our primary caution to investigators wishing to apply this LCMV QPCR method is to be extremely conscientious regarding negative control samples. QPCR is extremely sensitive, and cross-contamination is a continuous problem for any QPCR assay, particularly in cases like LCMV where a researcher would like to be able to detect the virus accurately over a range of 10^8 (compared to cellular RNAs, where it is rare to need more than a 100-fold range). As such, several sets of precautions must be put in place (described in Methods) to avoid being misled by inevitable periodic contaminations of samples at levels even as low as 0.0001%.

Acknowledgements

We thank Rafi Ahmed and Juan Carlos de la Torre for gifts of viruses and reagents. We thank Nathalie Droin, Sara McBride, Dr. Luca Guidotti, and Dr. Matteo Iannacone for initial assistance with QPCR. We thank Hung Tran for technical assistance and LCMV sequencing. This work was funded in part by a Cancer Research Institute Investigator Award to SC and a Pew Scholar Award to SC.

References

- Ahmed R, Salmi A, Butler LD, Chiller JM, Oldstone MB. Selection of genetic variants of lymphocytic choriomeningitis virus in spleens of persistently infected mice. Role in suppression of cytotoxic T lymphocyte response and viral persistence. *J Exp Med* 1984;160:521–40. [PubMed: 6332167]
- Bachmann MF, Hunziker L, Zinkernagel RM, Storni T, Kopf M. Maintenance of memory CTL responses by T helper cells and CD40-CD40 ligand: antibodies provide the key. *Eur J Immunol* 2004;34:317–26. [PubMed: 14768036]
- Buchmeier, MJ.; Zajac, A. Lymphocytic Choriomeningitis Virus. In: Ahmed, R.; Chen, I., editors. *Persistent Viral Infections*. John Wiley and Sons; 1999. p. 575-605.
- Crotty S, Kersh EN, Cannons J, Schwartzberg PL, Ahmed R. SAP is required for generating long-term humoral immunity. *Nature* 2003;421:282–7. [PubMed: 12529646]
- Crotty S, McCausland MM, Aubert RD, Wherry EJ, Ahmed R. Hypogammaglobulinemia and exacerbated CD8 T-cell-mediated immunopathology in SAP-deficient mice with chronic LCMV infection mimics human XLP disease. *Blood* 2006;108:3085–93. [PubMed: 16788096]

- Graham DB, Bell MP, McCausland MM, Huntoon CJ, van Deursen J, Faubion WA, Crotty S, McKean DJ. Ly9 (CD229)-Deficient Mice Exhibit T Cell Defects yet Do Not Share Several Phenotypic Characteristics Associated with SLAM- and SAP-Deficient Mice. *J Immunol* 2006;176:291–300. [PubMed: 16365421]
- Klenerman P, Hengartner H, Zinkernagel RM. A non-retroviral RNA virus persists in DNA form. *Nature* 1997;390:298–301. [PubMed: 9384383]
- Lee KJ, Perez M, Pinschewer DD, de la Torre JC. Identification of the lymphocytic choriomeningitis virus (LCMV) proteins required to rescue LCMV RNA analogs into LCMV-like particles. *J Virol* 2002;76:6393–7. [PubMed: 12021374]
- Matloubian M, Kolhekar SR, Somasundaram T, Ahmed R. Molecular determinants of macrophage tropism and viral persistence: importance of single amino acid changes in the polymerase and glycoprotein of lymphocytic choriomeningitis virus. *J Virol* 1993;67:7340–9. [PubMed: 7693969]
- Matloubian M, Somasundaram T, Kolhekar SR, Selvakumar R, Ahmed R. Genetic basis of viral persistence: single amino acid change in the viral glycoprotein affects ability of lymphocytic choriomeningitis virus to persist in adult mice. *J Exp Med* 1990;172:1043–8. [PubMed: 2212940]
- Roberts TJ, Lin Y, Spence PM, Van Kaer L, Brutkiewicz RR. CD1d1-dependent control of the magnitude of an acute antiviral immune response. *J Immunol* 2004;172:3454–61. [PubMed: 15004145]
- Salvato M, Shimomaye E, Oldstone MB. The primary structure of the lymphocytic choriomeningitis virus L gene encodes a putative RNA polymerase. *Virology* 1989;169:377–84. [PubMed: 2705303]
- Salvato M, Shimomaye E, Southern P, Oldstone MB. Virus-lymphocyte interactions. IV. Molecular characterization of LCMV Armstrong (CTL+) small genomic segment and that of its variant, Clone 13 (CTL-). *Virology* 1988;164:517–22. [PubMed: 3259346]
- Salvato MS, Shimomaye EM. The completed sequence of lymphocytic choriomeningitis virus reveals a unique RNA structure and a gene for a zinc finger protein. *Virology* 1989;173:1–10. [PubMed: 2510401]
- Simon ID, Publicover J, Rose JK. Replication and propagation of attenuated vesicular stomatitis virus vectors in vivo: vector spread correlates with induction of immune responses and persistence of genomic RNA. *J Virol* 2007;81:2078–82. [PubMed: 17151110]
- Thomsen AR, Johansen J, Marker O, Christensen JP. Exhaustion of CTL memory and recrudescence of viremia in lymphocytic choriomeningitis virus-infected MHC class II-deficient mice and B cell-deficient mice. *J Immunol* 1996;157:3074–80. [PubMed: 8816417]
- Wherry EJ, Ahmed R. Memory CD8 T-cell differentiation during viral infection. *J Virol* 2004;78:5535–45. [PubMed: 15140950]
- Whitmire JK, Flavell RA, Grewal IS, Larsen CP, Pearson TC, Ahmed R. CD40-CD40 ligand costimulation is required for generating antiviral CD4 T cell responses but is dispensable for CD8 T cell responses. *J Immunol* 1999;163:3194–201. [PubMed: 10477587]
- Whitmire JK, Slifka MK, Grewal IS, Flavell RA, Ahmed R. CD40 ligand-deficient mice generate a normal primary cytotoxic T- lymphocyte response but a defective humoral response to a viral infection. *J Virol* 1996;70:8375–81. [PubMed: 8970958]

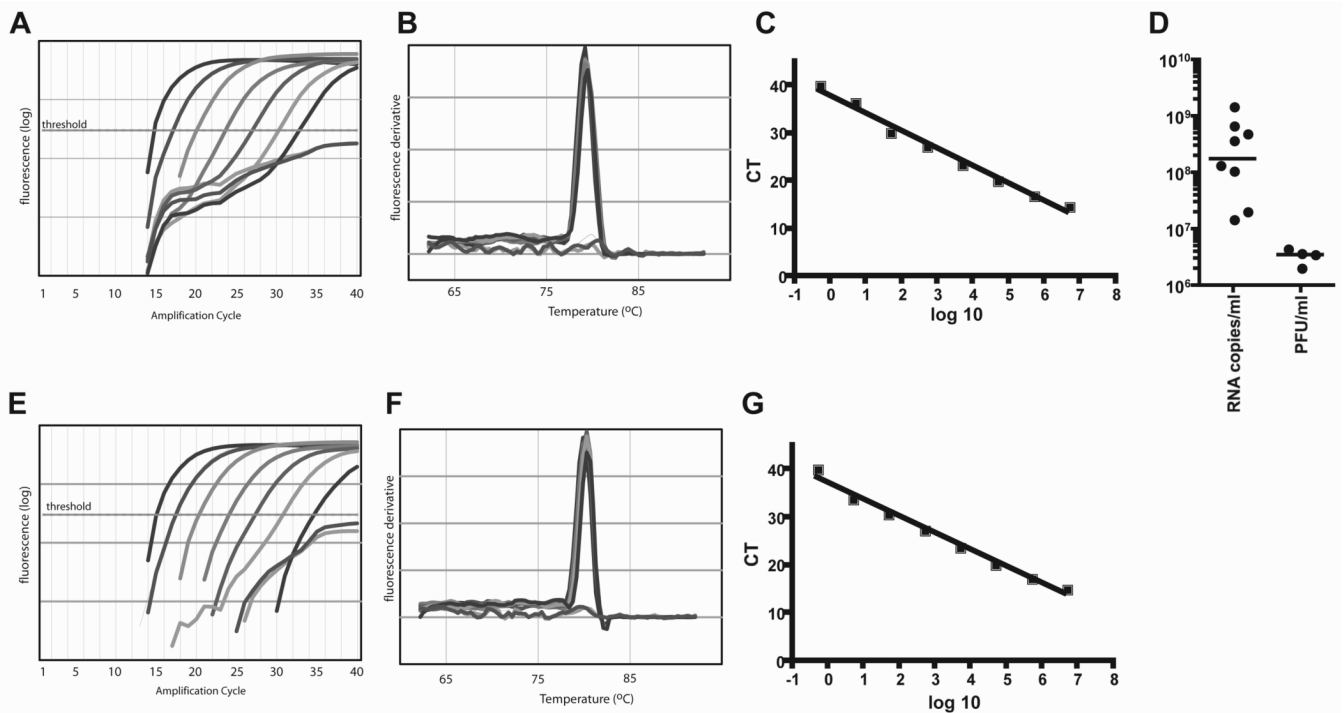


Figure 1. Quantitative LCMV RT-PCR (QPCR)

(a-d) NP primers. (e-g) GP primers. (a) QPCR LCMV NP standard curve using serial dilutions of an NP encoding plasmid. Dotted line indicates threshold used to establish a positive signal. Each curve is the amplification product from an amount of plasmid template 10-fold greater than the next sample to the right. (b) Melt curves of amplified NP PCR products from the standard curve samples, demonstrating the presence of a single amplification product with the expected melting temperature. (c) Quantitation of the NP standard curve. (CT = cycle threshold) (d) QPCR of LCMV_{arm} viral stock (LCMV RNA copies/ml), in comparison with conventional plaque assay (PFU/ml). (e) QPCR LCMV GP standard curve using serial dilutions of an GP encoding plasmid. Each curve is the amplification product from an amount of plasmid template 10-fold greater than the next sample to the right. (f) Melt curves of amplified GP PCR products from the standard curve samples, demonstrating the presence of a single amplification product with the expected melting temperature. Data is representative of more than three independent experiments. (g) Quantitation of the GP standard curve. (CT = cycle threshold).

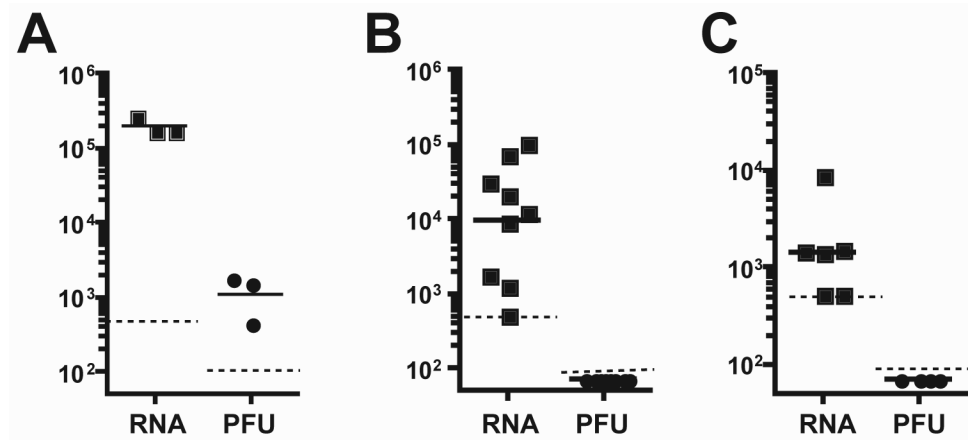


Figure 2. Serum viral loads in LCMV_{cl13} infected mice
 Comparison between QPCR (LCMV RNA copies/ml, “RNA”) and plaque assay (PFU/ml, “PFU”). Assays were run in parallel on samples divided into two aliquots. (a) Day 30 post-infection. (b) Day 60 post-infection. (c) Day 90 post-infection. Means are indicated by solid bars. Dashed lines indicate detection threshold for each assay. Data is representative of more than three independent experiments.

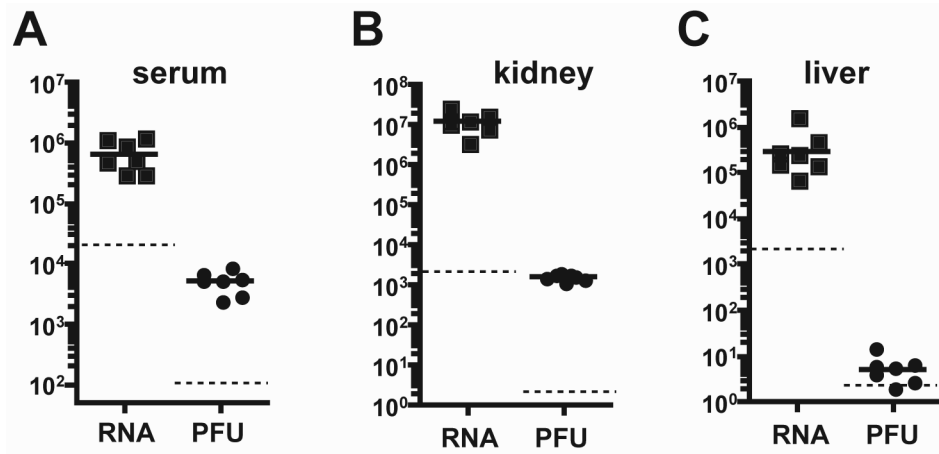


Figure 3. Serum and tissue viral loads in LCMV_{cl13} infected mice

Serum (a), kidney (b), and liver (c) samples were taken from a group of seven mice at day 30 after infection with LCMV_{cl13}. QPCR (LCMV RNA copies/ml, “RNA”) and plaque assay (PFU/ml, “PFU”) were directly compared. Assays were run in parallel on samples divided into two aliquots. Means are indicated by solid bars. Dashed lines indicate detection threshold for each assay. Data is representative of more than three independent experiments.

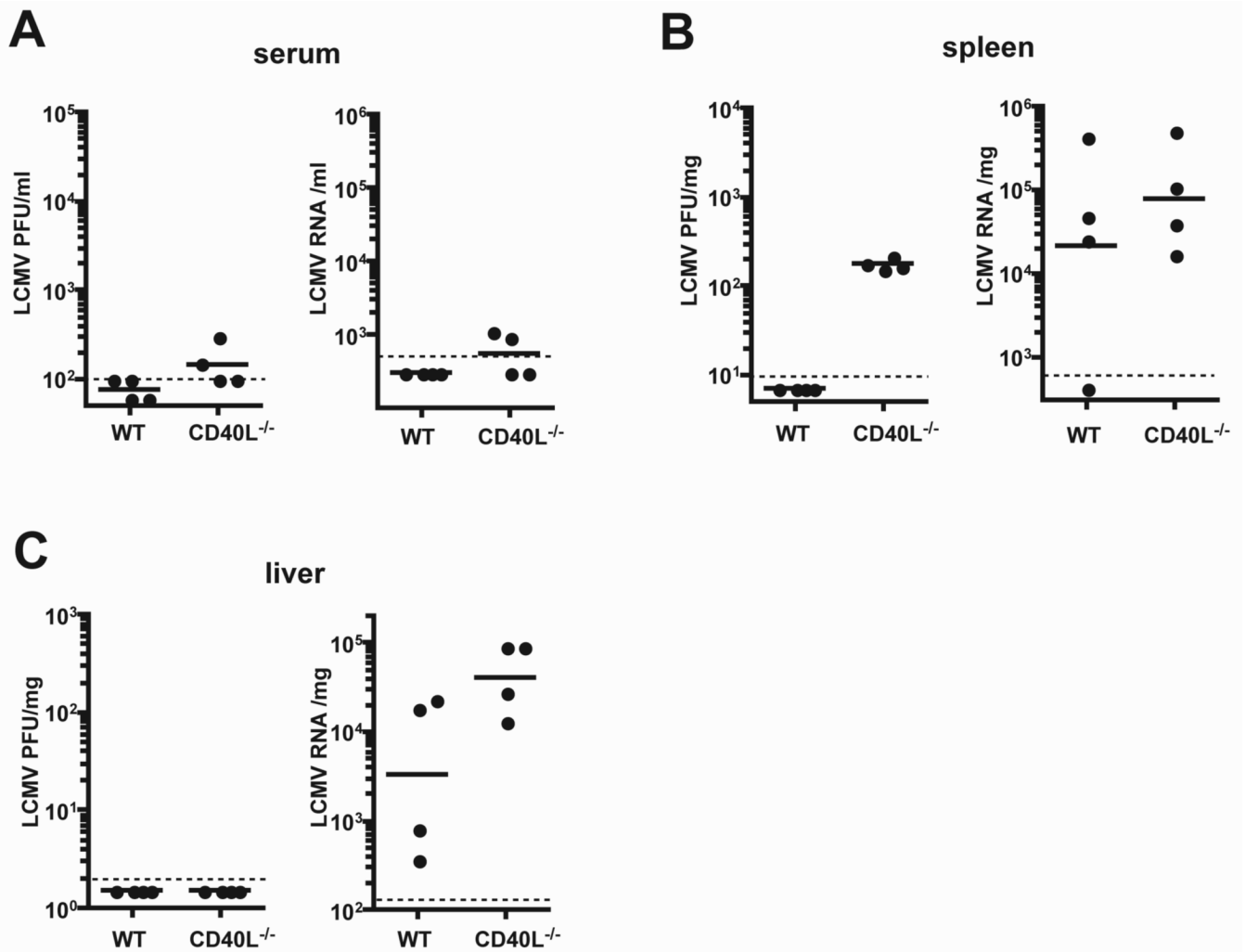


Figure 4. LCMV_{arm} viral loads in CD40L^{-/-} mice at day 8 postinfection
 Wildtype (WT) and CD40L^{-/-} mice were infected i.p. with LCMV_{arm}, and viral loads were measured at day 8 postinfection. QPCR (LCMV RNA copies/ml, “RNA”) and plaque assay (PFU/ml, “PFU”) were directly compared. Assays were run in parallel on samples divided into two aliquots. Means are indicated by solid bars. Dashed lines indicate detection threshold for each assay. (a) Serum. (b) spleen. (c) liver. Data is representative of two independent experiments.

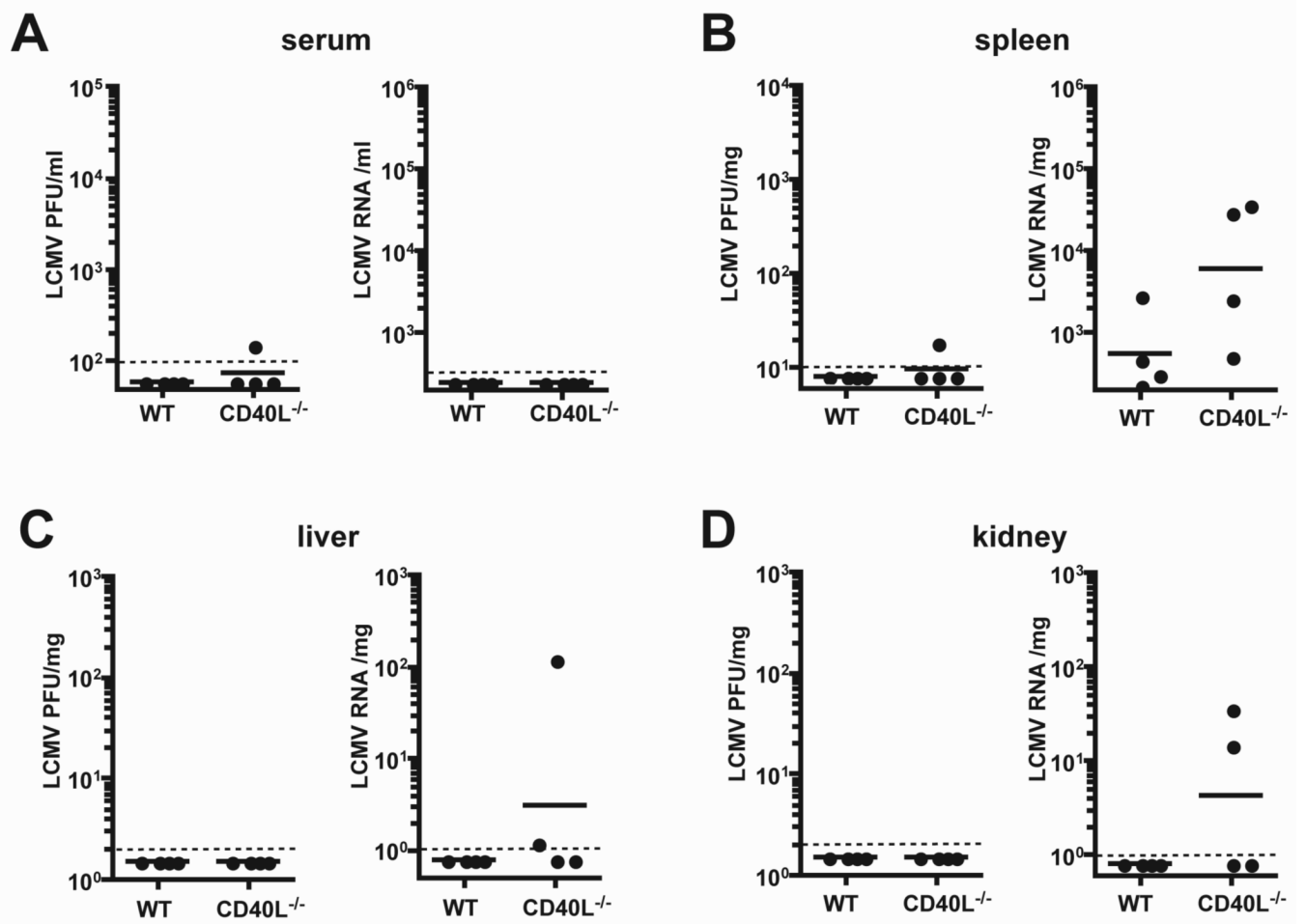


Figure 5. LCMV_{arm} viral loads in CD40L^{-/-} mice at day 30 postinfection
(a) Serum. **(b)** Spleen. **(c)** Liver. **(d)** Kidney. Assays were run as described in Figure 4. Data is representative of two independent experiments. Dashed lines indicate detection threshold for each assay, or the threshold is below the baseline shown.

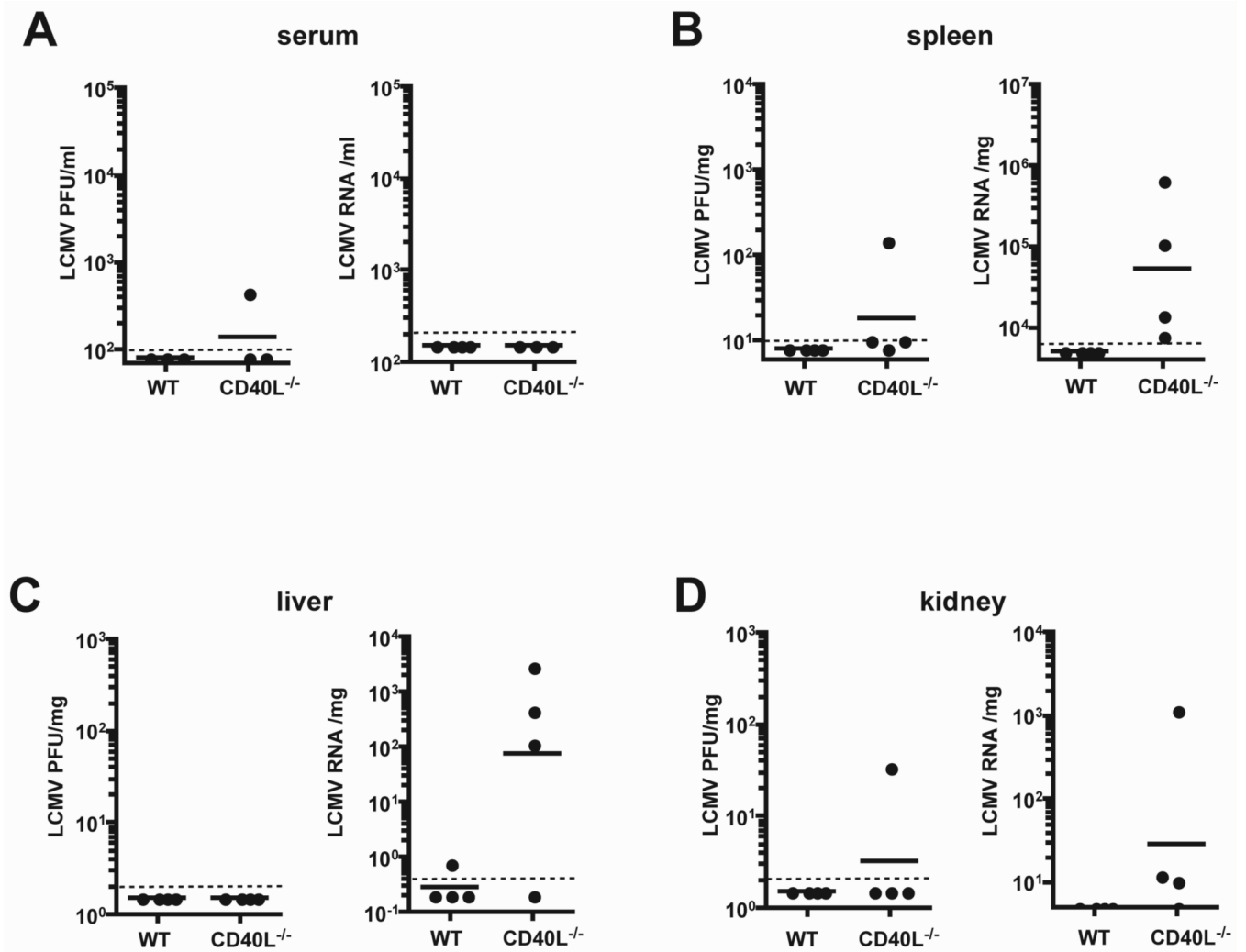


Figure 6. LCMV_{arms} viral loads in CD40L^{-/-} mice at day 90 postinfection
(a) Serum. **(b)** Spleen. **(c)** Liver. **(d)** Kidney. Assays were run as described in Figure 4. Dashed lines indicate detection threshold for each assay, or the threshold is below the baseline shown.

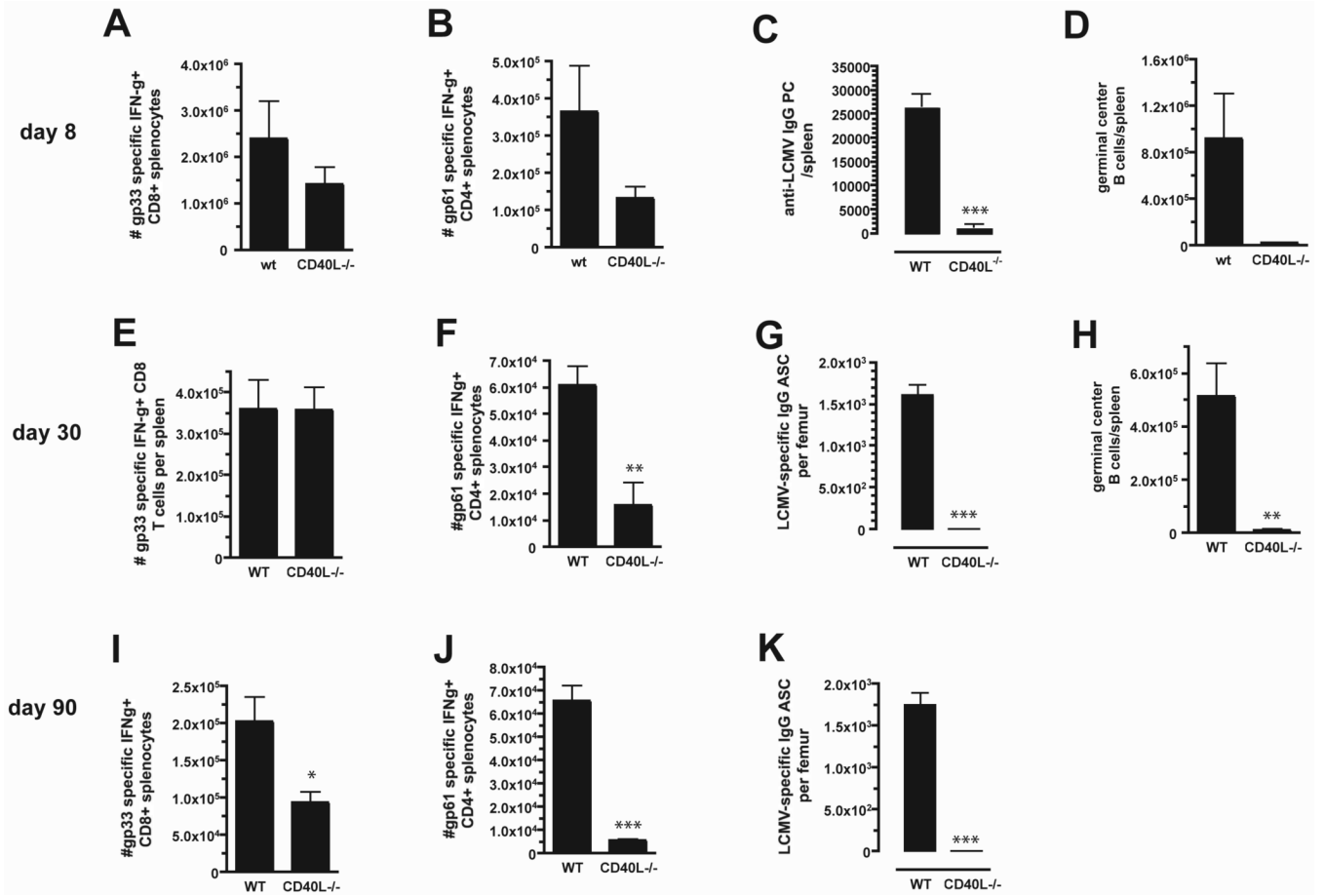


Figure 7. Immune responses in CD40L^{-/-} mice

LCMV-specific CD8 T cells (a,e,i), CD4 T cells (b,f,j), plasma cells (c,g,k), and germinal centers (d,h) were quantified in the wildtype (“WT”) and CD40L^{-/-} mice from Figures 4,5, and 6 at days 8 (a-d), 30 (e-h), and 90 (i-k) after infection with LCMV_{arm}. N = 4/group. * = P < 0.05. ** = P < 0.01. *** = P < 0.001.

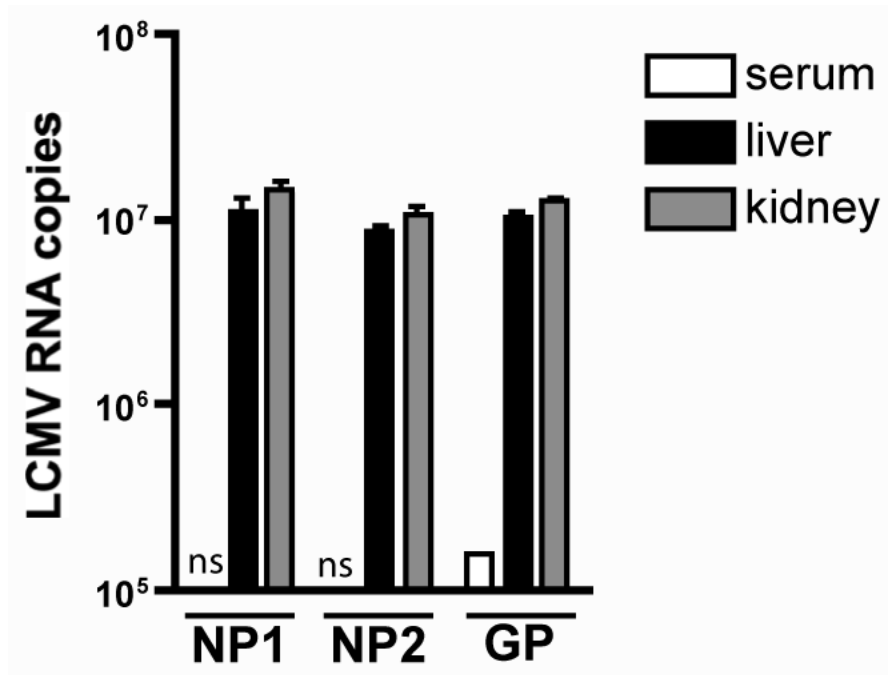


Figure 8. Comparison of primer pairs NP1 (original), NP2, and GP
 Serum, liver, and kidney samples were tested from two representative LCMV_{c113} infected mice at day 30 postinfection. (ns = nonspecific products, as determined by melt curve)

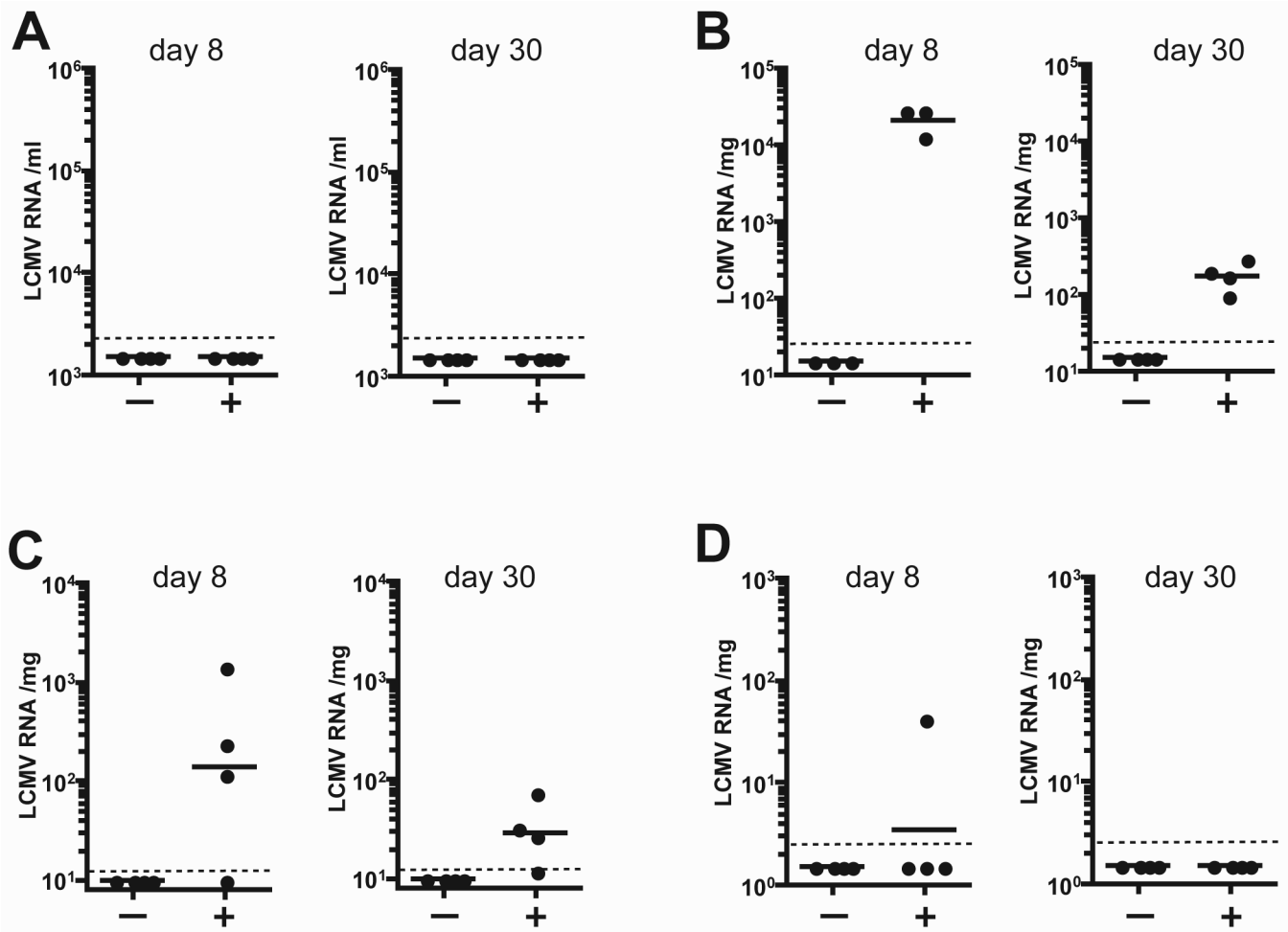


Figure 9. LCMV_{arm} viral loads, using GP primers

Wildtype mice infected with LCMV_{arm} were tested at day 8 and day 30 post-infection for LCMV using GP QPCR primers. Infected mice (“+”) were compared against uninfected mice (“-”) in all cases. (a) Serum. (b) Lymph node (inguinal). (c) Spleen. (d) Kidney. Dashed line indicates detection threshold.